Available online at www.sciencedirect.com
SCIENCE DIRECT
Biochemical Pharmacology 69 (2005) 415–423
Biochemical Pharmacology
www.elsevier.com/locate/biochempharm

Directional trans-epithelial transport of organic anions in porcine LLC-PK1 cells that co-express human OATP1B1 (OATP-C) and MRP2

Kevin J. Spears[a], Jillian Ross[a], Alasdair Stenhouse[a], Clive J. Ward[a], Lay-Beng Goh[a], C. Roland Wolf[a], Paul Morgan[b], Andy Ayrton[c], Thomas H. Friedberg[a,*]

[a]*Biomedical Research Centre, University of Dundee, Ninewells Hospital and Medical School, Dundee DD1 9SY, UK*
[b]*Pfizer Global Research, Sandwich, Kent CT13 9NJ, UK*
[c]*GlaxoSmithKline, The Frythe, Welwyn, HERTS AL6 9AR, UK*

Received 3 August 2004; accepted 29 September 2004

Abstract

The transcellular transport of many compounds, which cannot readily cross the lipid bilayer, is mediated by drug uptake and efflux transporters. Human OATP1B1 and MRP2 have been implicated in the hepato-biliary transport of many endogenous and exogenous compounds. Here, we have established epithelial porcine kidney LLC-PK1 derived cell lines, that express both transporters in a polarized fashion, as a model to predict hepato-biliary transport. Immunological identification of OATP1B1 in the recombinant cell lines was greatly facilitated by its C-terminal tagging with a peptide sequence derived from hemagglutinin (HA) avoiding the generation of OATP1B1 specific antibodies. Importantly, the tag did not interfere with the functionality of the transporter. Compared to LLC-PK1 cells and cells which expressed only OATP1B1, the cell line that co-expressed MRP2 and OATP1B1 displayed high directional basolateral-to-apical transport of 17β-estradiol–17β-glucuronide and estrone-3-sulfate. Dehydroepiandrosterone sulfate already displayed a significant basolateral-to-apical transport in the parental cell line, which was further stimulated upon expression of both transporters. Transcellular flux of all steroid conjugates in the opposite direction (apical-to-basolateral) was much lower. By employing this cellular model we were able to demonstrate for the first time that OATP1B1 together with MRP2 mediates the trans-cellular transport of rifampicin. It is anticipated that the models established herein will greatly facilitate the identification of transporters involved in the disposition of novel drug candidates.

Keywords: Drug transport; Preclinical drug development; Organic anion transport; Mutidrug resistance

1. Introduction

Hepato-biliary transport, influences the rate of biliary secretion of many drugs. While lipophilic compounds enter hepatocytes usually by passive diffusion, amphipathic molecules frequently requires carrier-facilitated uptake. Subsequently, the compounds are metabolised to more hydrophilic molecules, if required, and subsequently excreted into the bile [1].

Human OATP1A2 (also termed OATP-A), hepatic OATP1B1 (also termed OATP-C or LST-1) and OATP1B3 (OATP-8) are the key drug uptake transporters with OATP1B1 and OATP1B3 being located at the basolateral membrane of the hepatocyte ([2], this review gives also a comprehensive update on the recent OATP nomenclature). OATPs mediate the Na^+-independent, saturable transport of differently charged amphipathic compounds such as bile acids, bromosulphophthalein (BSP), unconjugated and conjugated steroid hormones such as 17β-estradiol–17β-glucuronide ($E_2$17βG), as well as xenobiotics [2]. Pharmaceutical drugs which are taken up by OATP1B1 include the anti-hyperlipodemic drugs pravastatin [3], the quinolone derivative sparfloxacine, the anti-histamine

Abbreviations: BSA, bovine serum albumin; DHEAS, Dehydroepiandrosterone-sulfate; $E_2$17βG, 17β-estradiol–17β-glucuronide; E_1S, estrone 3-sulfate; FBS, fetal bovine serum; HA, hemagglutinin; HBSS, Hanks balanced salt solution; MDCK, Mardin Darby canine kidney cells; MDR, multidrug resistance protein; MRP, multidrug resistance-associated protein; OATP, organic anion transporting polypeptide

* Corresponding author. Tel.: +44 1382 660111x33486; fax: +44 1382 669993.
E-mail address: t.h.friedberg@dundee.ac.uk (T.H. Friedberg).

0006-2952/$ – see front matter © 2004 Elsevier Inc. All rights reserved.
doi:10.1016/j.bcp.2004.09.026

fexofenadine (reviewed in [1]) and the anti-hypertensive compound temocaprilat [4]. It is important to note that polymorphisms in OATP1B1 affect its activity towards pravastatin and rifampicin [3,5].

MDR1 (P-glycoprotein) and MRP2 are key human hepatic membrane drug efflux transporters (reviewed by [6]). Although substrates of MRP1 and MRP2 are mainly bulky, conjugated anions, these proteins also transport some non-conjugated drugs that are substrates of MDR1. For example, vinblastine, a well-known substrate of MDR1 is also transported by MRP1 [7] and MRP2 [8]. MRP2 is thought to be the main hepatic efflux pump for amphipathic drugs or drug metabolites and is located at the apical site of the hepatocyte, thus facing the biliary lumen. Furthermore MRP2 has been shown to efflux conjugates of endogenous compounds such as $E_2$17βG or glutathione conjugates of leukotrienes (e.g., LTC_4). Several of the compounds which are substrates of human OATPs are also effluxed by rodent or human MRP2. Thus OATP1B1 or OATP1B3 in conjunction with MRP2 may have a key-role in the hepato-biliary disposition of many endogenous and exogenous compounds or their conjugates [9].

As the role of transport-mediated processes in drug disposition and elimination emerges, it is important to realise that species differences occur between animals and humans, particularly for drug clearance and excretion. For some drugs, which are cleared unchanged primarily by hepato-biliary excretion, large differences occur which are not attributable to protein binding differences (reviewed in: [1]). For example there is a 20- and 7-fold over-estimation of human clearance for susalimod and napsagatran, respectively, from animal clearance data. Similarly MRP2-mediated hepato-biliary transport of temocaprilat displays large differences between human, mouse, rat, guinea pig, rabbit, and dog. These effects could be caused by inter-species differences in the substrate specificity or in the level of the various transporters. For example, species differences in the V_{max} and possibly also in the K_m of MRP2 for temocaprilat, may explain why this compound is mainly excreted into the bile in humans but not in the rat.

Given the large inter-species variation in the hepato-biliary excretion of some drugs, the availability of in vitro cellular systems to predict carrier-mediated drug disposition in man would facilitate pre-clinical drug development. Human hepatocytes are not suitable as a model since they are difficult to obtain and because MRP2 and OATPs are de-regulated in vitro [10]. Similarly, some OATPs are down-regulated in human hepatoma cells with the liver specific OATP1B1 being undetectable in HepG2 cells [11]. Here we describe the establishment and characterisation of porcine kidney cell line LLC-PK1 derived cells that co-express OATP1B1 and MRP2 as a model for the vectorial hepatic drug transport in humans.

2. Materials and methods

2.1. Chemicals

[^{3}H] 17β-Estradiol–17β-glucuronide, [^{3}H] estrone sulphate and [^{3}H] DHEAS were purchased from NEN Life Science Products Inc. The specific radioactivity of these substrates as employed in the assays is given below. G-418 (Geneticin) sulphate was purchased from Gibco-BRL. Zeocin was purchased from Invitrogen. Monoclonal antibodies against MRP2 (M_2III-6) raised in mouse were purchased from Alexis Corporation Ltd. and monoclonal antibodies raised in rat against the hemagglutinin-tag (3F10) from Roche Molecular Biochemicals. All other non-radioactive chemicals were purchased from Sigma.

2.2. Isolation of cDNAs and cloning into expression vectors

We employed a method that allowed the detection of recombinant OATP1B1 expression in the absence of suitable anti-transporter antibodies. For this approach, we expressed OATP1B1 modified with a short peptide sequence derived from hemagglutinin (HA). The tagged protein was then detected employing anti-HA tag antibodies. Initially, the coding region of the OATP1B1 cDNA was isolated by RT-PCR and verified by DNA-sequencing to be identical to the published sequence (GenBank accession no. AF060500). Subsequently, 3′ HA-tagged OATP1B1 cDNA was isolated by RT-PCR employing the OATP1B1 cDNA as template as follows: The HA-tag comprising 27 nucleotides (5′-TAC CCA TAC GAC GTA CCA GAC TAC GCA-3′) encoding the amino acids YPYDVPDYA, was incorporated just before the stop codon, while two linkers, *Xho*I and *Xba*I sites, were incorporated at the 5′ and 3′ ends of the cDNA, respectively. This cDNA was cloned, after confirmation by sequencing, into the pcDNAzeo3.1 expression vector (Invitrogen BV, Groningen, The Netherlands) at the *Xho*I and *Xba*I sites.

The coding region of the human MRP2 cDNA was isolated by RT-PCR employing primers that introduced at the 5′end of the cDNA a Hind III site and at the 3′-end a Not I site. The PCR product was cloned into the pcDNAneo3.0 expression vector (Invitrogen BV, Groningen, The Netherlands) at the Hind III and Not I sites. The sequence of the MRP2 cDNA was verified by DNA-sequencing to be identical to the published sequence (accession no. U63970s).

2.3. Cell culture and transfection study

LLC-PK1 porcine kidney cells (obtained from ATCC) were cultured in Medium 199 (Gibco BRL) supplemented with 10% (v/v) fetal bovine serum (FBS), 50 units/ml penicillin and 50 μg/ml streptomycin (defined as growth medium) at 5% CO_2 and 37 °C. The LLC-PK1 cells were

transfected with plasmid DNA using calcium phosphate co-precipitation kit (Gibco BRL). The cells were grown at a density of 1×10^6 cells per 10 cm dish, in 10 ml growth medium at 37 °C, 5% CO_2 for 24 h. Three hours prior to transfection, fresh growth medium was added. For each transfection reaction, 20 μg ethanol precipitated DNA was used. Following 24 h-exposure to the calcium phosphate/DNA co-precipitate, cells were propagated in growth medium for 48 h, before being split 1:1000 into the same medium containing either Zeocin and/or G-418 both at 700 μg/ml.

Initially the OATP1B1 cDNA was transfected into LLC-PK1 cells. After 10–15 days Zeocin selection, single clones were transferred to 24 well-culture plates using paper cloning-discs (Sigma, Dorset, UK), soaked in trypsin. Cells were given 24 h recovery in growth medium before adding selective antibiotics. Clones were expanded and analysed for the expression of OATP1B1 initially by immunoblotting and immunofluorescence microscopy. Subsequently, cell lines that expressed OATP1B1 homogeneously were transfected as described above with the expression vector carrying the MRP2 cDNA. Clones that were resistant to both Zeocin and G-418 were characterized by immunoblotting and immunofluorescence for the expression of both human transporters.

2.4. Immunoblot analysis

For immunoblot analysis, crude total cell extracts were prepared from LLC-PK1 cells by detaching cells (2.5% trypsin/0.01% EDTA) and re-suspending in cell suspension buffer (sodium phosphate (10 mM), EDTA (1 mM), DTT (5 mM), 1% PMSF, 1% Protease inhibitors, pH 7.4). Cell extracts were sonicated and stored at −80 °C. Protein concentrations were determined using Bio-rad protein assay reagent (purchased from Bio-rad Labs), with bovine serum albumin (BSA) as the standard.

For immunoblot analysis, 20 μg of crude cell extract was analysed, without prior heat-denaturation, by immunoblotting as described [12] employing SDS-PAGE in 7.5% polyacrylamide gels. The molecular weight was determined using prestained protein markers (Amersham International). The blots were reacted with either the anti-HA monoclonal antibody at a 1:2000 dilution or a polyclonal rabbit antibody directed against the C-terminus of OATP1B1 (generous gift by D. Keppler, Heidelberg, [13]) in order to visualise OATP1B1, or with the anti-MRP2 antibody at a 1:500 and a 1:200 respectively dilution. After washing, the blots were reacted with horseradish peroxidase coupled secondary anti-mouse or anti-rabbit respectively antibodies (Sigma). Subsequently, the blot was washed and developed employing the ECL Plus Western blotting Kit (Amersham International PLC).

2.5. Confocal laser scanning microscopy

Transfected LLC-PK1 cells were grown in growth medium (composition as above) on transwell membrane inserts (Corning Incorporated) for 3 days to confluency. After fixation in PBS containing 4% paraformaldehyde and permeabilisation in PBS containing 0.3% Triton X-100, the cells were incubated with the rat monoclonal anti-HA-tag antibody (diluted 200-fold in PBS containing 1% BSA) and the mouse anti-MRP2 antibody (diluted 50-fold in PBS containing 1% BSA) for 1 h at room temperature. Secondary antibodies used were anti-mouse IgG Alexa Fluor® 594 and anti-rat Alexa Fluor 488 (both Molecular Probes). Subsequently, the membrane was cut from the filter cup insert and mounted on a glass slide employing hydromount mounting media. Confocal laser scanning microscopy was performed with a LSM 510 microscope (Zeiss GmbH).

2.6. Transcellular transport assay for organic anions

Transfected LLC-PK1 cells were seeded into 6-well Transwell plates (Corning Costar, Bucks, UK) at a density of 1×10^6 cells per well and grown for 4 days at 5% CO_2, 37 °C in growth medium. The integrity of the monolayer was verified for each well using lucifer yellow (LY) as described [14]. The accepted level for LY permeability was 15 nm/s [14]. For transport assays, the cells were washed three times and preincubated with Krebs–Henseleit buffer (Sigma) with the addition of $NaHCO_3$ (2.1g/l), $CaCl_2$ (dihydrate) (0.373 g/l), adjusted to pH 7.4. This medium did not contain any serum, which may sequester substrates as discussed [15]. The radiolabelled substrates were employed at a specific radioactivity of 2–3 Ci/mmol. The experiments were initiated by replacing the preincubation buffer at either the basal or apical side of the cell layer with Krebs–Henseleit buffer containing [^{3}H] $E_2$17βG, [^{3}H] E_2-S, [^{3}H] DHEAS each 1 μM or Rifampicin (50 μM). The cells were incubated at 37 °C, and aliquots of buffer were taken from each compartment at several time points as indicated in the figure legends. Radioactivity in 25 μl of buffer was measured in a liquid scintillation counter (LS 6500, Beckmann Instruments Inc, Fullerton, CA) after addition of scintillation fluid (Fisher Chemicals). The transport of rifampicin was assayed by measuring absorption at 475 nm respectively. Transport assays were carried out in triplicate and values are expressed as S.D. ± means. Statistical analysis for the transport of rifampicin across the various cell lines was performed using the paired *t*-test ($n = 3$).

2.7. Mass-spectroscopic analysis of estrone-sulfate following its transcellular transport

Transcellular transport of unlabelled E_2-S (10 μM) from the basal to the apical site was carried out as described above. Substrate accumulating at the apical site of the transwell was analysed further by mass spectroscopy. The samples or standard estrone-3-sulfate (1.0 μM) were extracted twice by shaking with 1 ml ethyl acetate for approximately 5 min. The organic layers were removed, combined and dried under

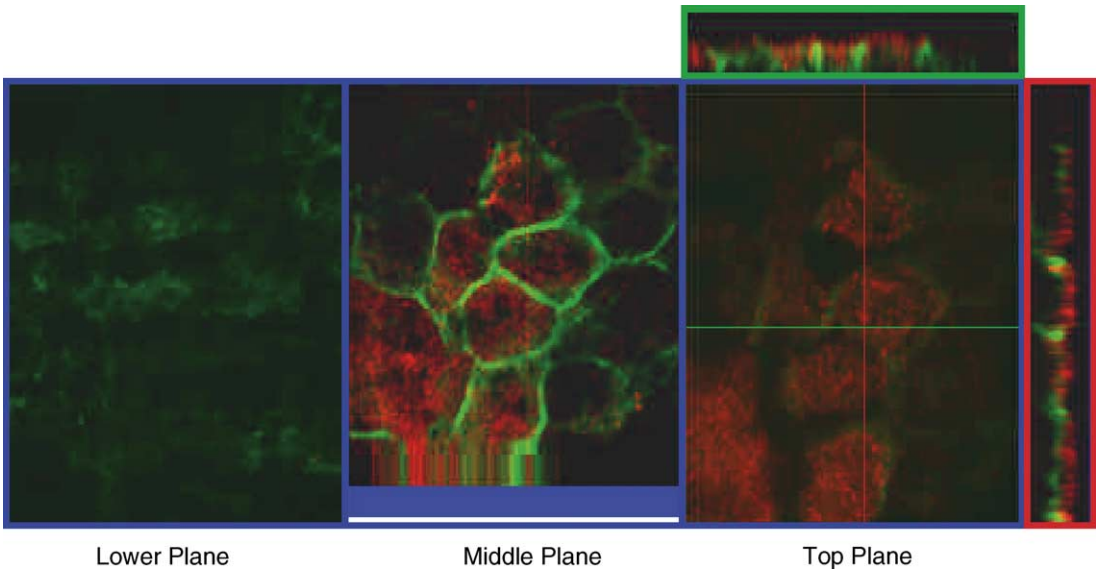

Fig. 1. Confocal laser scanning microscopy for stably transfected LLC-PK1 cells. Immunolocalisation of HA-tagged OATP1B1 (OATP-C) and MRP2 in LLC-PK1 cells by confocal microscopy were carried out as described in Section 2. The signal obtained for MRP2 is red whereas that for OATP1B1 is green. Views were taken in the lower, the middle and the top plane. The two scans taken for the *z*-stacks along the *x* and the *y*-axis are given by red and green bars. (For interpretation of the references to colour in this figure legend, the reader is referred to the web version of the article.)

a stream of dry nitrogen at room temperature. Dried extracts were resuspended in 50 μl methanol prior to analysis. Samples were analysed by liquid chromatography/hybrid time-of-flight mass spectrometer (Q-TOF Micro, Micromass) with electrospray ionisation.

3. Results

3.1. Expression of OATP1B1 and MRP2 in LLC-PK1 cells

Initially cell lines that expressed OATP1B1 were established. Immunological identification of these cells was facilitated by the incorporation of a HA-tag at the C-terminus of OATP1B1. Cells which expressed this uptake transporter throughout the population were further transfected with the MRP2 cDNA. Fig. 1 displays confocal laser-scanning microscopy of cells that co-express MRP2 and OATP1B1 and which had been grown on a transwell membrane. In the horizontal view MRP2 (red) is clearly localised in the apical membrane (strong staining in the top horizontal plane), whereas the baso-lateral localisation of OATP1B1 (green) can be best seen in the *y*–*z* stack, where in some parts the staining of OATP runs parallel to and below the staining for MRP2. Neither in the horizontal nor in the vertical view is there any evidence for colocalisation of OATP1B1 and MRP2.

As revealed by immunoblotting, anti-HA antibodies yielded no signal with parental LLC-PK1 cells while anti-MRP2 antibodies gave a faint signal (Fig. 2a and c). Cells that were transfected with OATP1B1 (termed LLC-OATPC) yielded a strong signal for this protein but a faint staining for MRP2, whereas cell lines that were transfected with both cDNAs stained strongly for both MRP2 and OATP1B1 (Fig. 2a and c). These cells were termed LLC-OATPC/MRP2. Immunoblot analysis was also carried out to compare the levels of the recombinant transporters in LLC-OATPC/MRP2 cells with those in human hepatocytes and HepG2 cells (Fig. 2b and d). In this experiment (Fig. 2b) antibodies directed against the C-terminus of OATP1B1 (generous gift by D. Keppler, Heidelberg, [13]) instead of antibody directed against the HA-tag, were used as primary antibodies. The anti-OATP1B1 antibodies stained proteins migrating at about 84 kDa and 58 kDa. A stronger signal was seen for the proteins migrating at about 84 kDa in LLC-OATPC/MRP2 cells compared to human hepatocytes. As expected, a weak signal was obtained with HepG2 cells. The level of MRP2 in LLC-OATPC/MRP2 cells was distinctly higher than that in hepatocytes and similar to the level in HepG2 cells (Fig. 2d).

3.2. Transcellular transport $E_2$17βG across cell monolayers

Fig. 3 displays the transcellular transport of $E_2$17βG in the basolateral-to-apical (filled symbols) and in the reverse direction (open symbols) in several cell lines. In initial experiments (data not shown), it was found that the total cellular protein per well was by a factor of less than 1.5-fold different between the various cell lines, provided that each well contained a tight monolayer of cells, as assessed by the lucifer yellow assay. Thus the values for the transcellular transport of substrates were expressed as pmol substrate transported per cm^2. It is important to note that parental LLC-PK1 and mock-transfected LLC-PK1

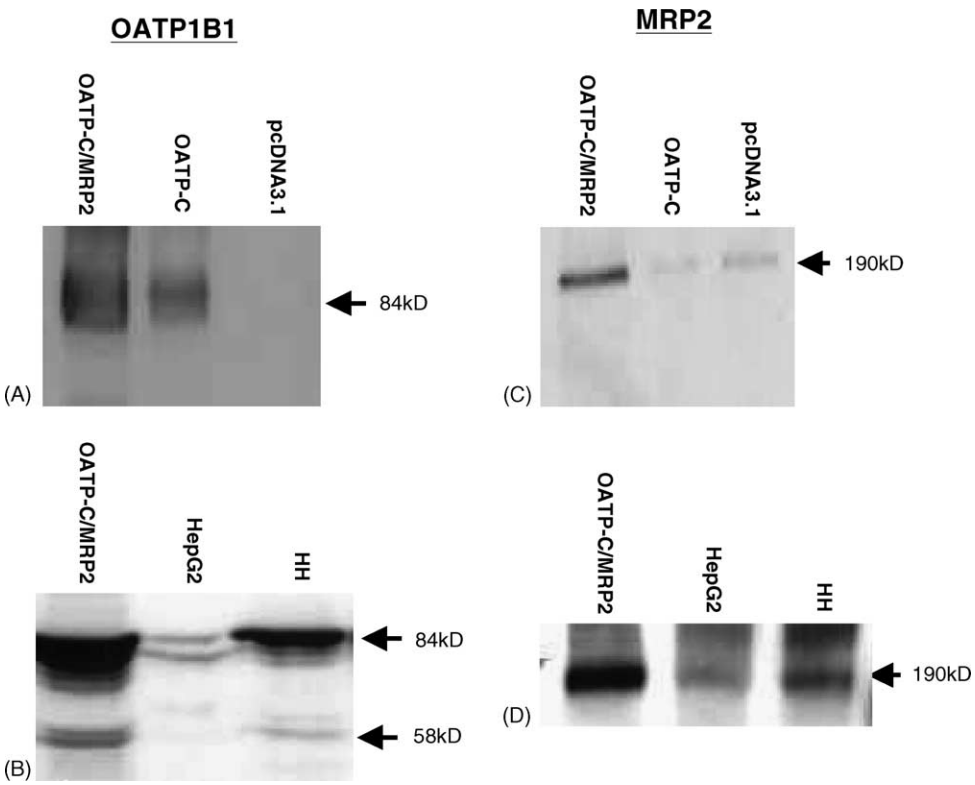

Fig. 2. Western blot analysis for OATP1B1 and MRP 210 μg of crude cell extracts from LLC-PK1 cells transfected either with empty vector (pcDNA3.1), or HA-tagged OATP1B1 (OATPC) or both HA-tagged OATP1B1 and MRP2 (OATPC/MRP2) were analysed by SDS-PAGE (7.5% resolving gel) followed by immunoblotting. (a) OATP1B1 was detected by monoclonal antibody against the HA-tag. (c) MRP2 was detected by a monoclonal antibody against the carboxyl terminus of human MRP2. (b) and (d) for comparison, lysate of the cell line co-expressing OATP1B1 and MRP2 was also analysed by immunoblotting together with lysates prepared either from HepG2 cells or human hepatocytes (HH). In this case polyclonal antibodies directed against the C-terminus of OATP1B1 (b) or the monoclonal antibody against human MRP2 (d) were used as primary antibodies.

both displayed very little vectorial transport. LLC-OATPC cells transported the substrate in the basal-to-apical direction distinctly faster than in the opposite direction. Basolateral-to-apical transport was strongly increased upon additional expression of MRP2 being at least 20-fold higher than in the reverse direction (10 pmol/(cm^2 h) versus 0.5 pmol/(cm^2 h)). It is important to note that co-expression of both transporters did not increase the apical-to-basolateral transport compared to that found in the parental cell lines. In LLC-OATPC and LLC-OATPC/MRP2 cells, basolateral-to-apical transport did not decrease with time for at least 60 min.

3.3. Transcellular transport E_1S and DHEAS across cell monolayers

Transcellular transport of E_1S in both directions was low in LLC-PK1 cells (Fig. 4). A lack of vectorial transport was seen in LLC-OATPC cells. At the 90 min timepoint a small preferential basolateral-to-apical transport was noted. LLC-OATPC/MRP2 cells diplayed a much higher basolateral-to-apical than apical-to-basolateral transport. However, unlike the transport of $E_2$17βG, the transport of E_1S showed a plateau after 30 min. Given this unusual time-course, we investigated the possibility that E_1S was metabolised within the cells. By employing mass-spectroscopic analysis, we verified that the compound transported from the basolateral to the apical site was indeed only E_1S and not a metabolite that may have been formed intra-cellularily (data not shown).

We also investigated the vectorial transport of another sulfated steroid, namely DHEAS (Fig. 5). In this case, LLC-PK1 cells already showed a basolateral-to-apical transport, which was clearly higher than in the opposite direction. Upon expression of OATP1B1, only a small increase of both the basolateral-to-apical and the apical-to-basolateral transport occurred. LLC-OATPC/MRP2 cells displayed a basolateral-to-apical transport, which was approximately 2-fold higher than in LLC-OATPC cells (1.3 pmol/(cm^2 h) versus 0.7 pmol/(cm^2 h)) and 3-fold higher than in LLC-PK1 cells (1.3 pmol/(cm^2 h) versus 0.4 pmol/(cm^2 h)). Apical-to-basolateral flux of DHEAS was similar in both LLC-OATPC and LLC-OATPC/MRP2 cells.

3.4. Transcellular transport of rifampicin across cell monolayers

Expression of OATP1B1 in LLC-PK1 cells did not increase the basolateral-to-apical transport of the antibiotic

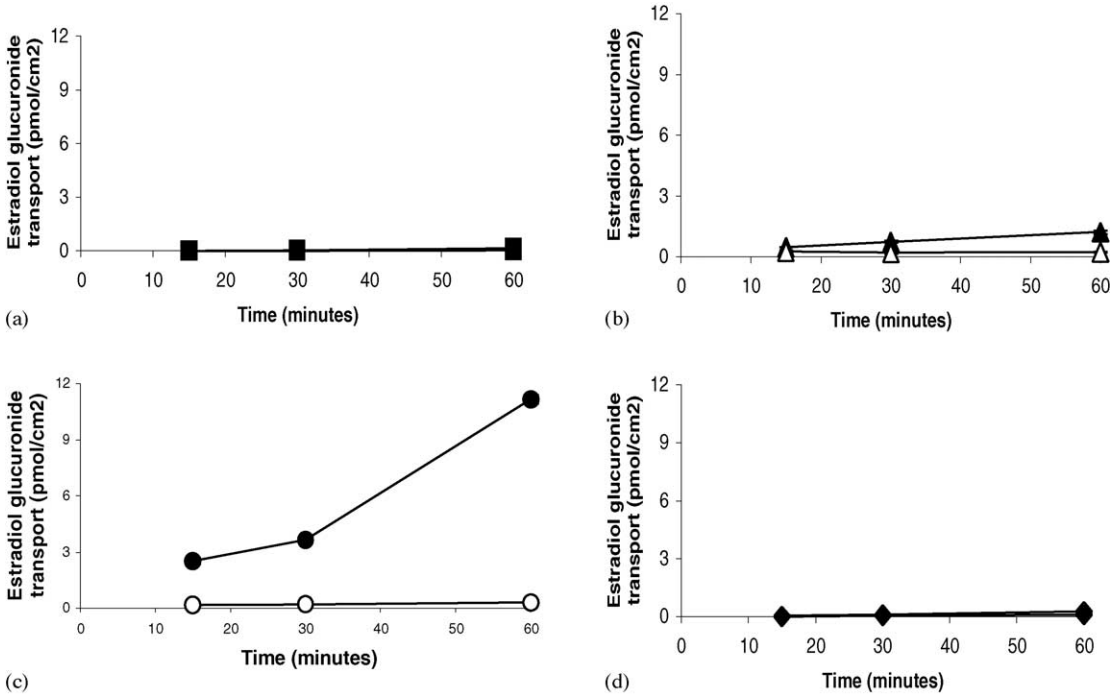

Fig. 3. Time profiles for the transcellular transport of estradiol glucoronide across LLC-PK1 monolayer. Transcellular transport of [^{3}H]$E_2$17βG (1 μM, specific activity: 2.025 Ci/mmol)) across LLC-PK1 monolayers expressing (c) OATP1B1, (d) both MRP2 and OATP1B1 compared with (a) untransfected LLC-PK1 cells and (b) mock-transfected LLC-PK1 cells. Open and closed circles represent the transcellular transport in the apical-to-basal and basal-to-apical directions, respectively. Each point and error bar represents the mean ± S.E. of three determinations. Where error bars are not shown, the S.E. was contained within the limits of the symbol.

rifampicin compared to parental LLC-PK1 and mock transfected LLC-PK1 (Fig. 6). All three cell lines showed a moderately higher basolateral-to-apical than apical-to-basolateral transport. However, in LLC-OATPC/MRP2 cells the basolateral-to-apical transport was 8-fold higher than in the parental cells and 6-fold higher than the flux in the opposite direction. In this cell line, however, the transport of rifampicin in the apical-to-basolateral direction was also elevated slightly compared to that found with the parental cells.

4. Discussion

In the present study we have established porcine kidney derived epithelial cell lines that express either the hepatic organic anion uptake transporter OATP1B1 alone or in combination with the hepatic efflux pump MRP2. Initially, both LLC-PK1 and MDCKII cells were chosen as recipient cell lines as both porcine and canine respectively are well established polarized kidney cell lines. Furthermore, we had previously shown that both cell lines were devoid of OATP1B1 and OATP1A2 and expressed very low levels of MRP2 [16]. Even though, we obtained several MDCKII derived cell lines that co-expressed MRP2 and OATP1B1 as evidenced by immunoblotting and immunofluorescence, none of them displayed preferential basolateral-to-apical transport of $E_2$17βG (data not shown). Instead, expression of these transporter in MDCK cells resulted in a enhanced transport of this substrate in both directions unlike the polarised transport seen with several LLC-PK1 cell lines (data not shown) in the present study. Of these only one was characterized in detail (see Section 3). The reasons for the differences seen between the recombinant MDCKII-derived cell lines and those established from LLC-PK1 cells are not known. However, it should be noted that during our work was in progress, MDCKII derived cell lines that co-expressed MRP2 together with either OATP1B1 or OATP1B3 have been established and showed directional transport of organic anions [15,17]. MDCK cells have also been used to express other transporter proteins [18].

Immunological identification of recombinant OATP1B1 in LLC-PK1 cells (Figs. 1 and 2a) was greatly facilitated by the addition of a C-terminal HA-tag. Antibodies against this tag are commercially available and have been shown to specifically recognize this epitope and not any other cellular protein. In some immunoblots (see Fig. 2a) the signal obtained for the glycosylated form of OATP1B1 (84 kDa) was fuzzy, as would be expected for glycosylated proteins. The de-glycosylated form of OATP1B1 (58 kDa) was only detected in the experiment displayed in the lower panel of Fig. 2b, which however already yielded a much stronger signal for the glycosylated OATP1B1, compared to the signal obtained in the experiment displayed in Fig. 2a. Analysis of parental LLC-PK1 cells by immunoblotting

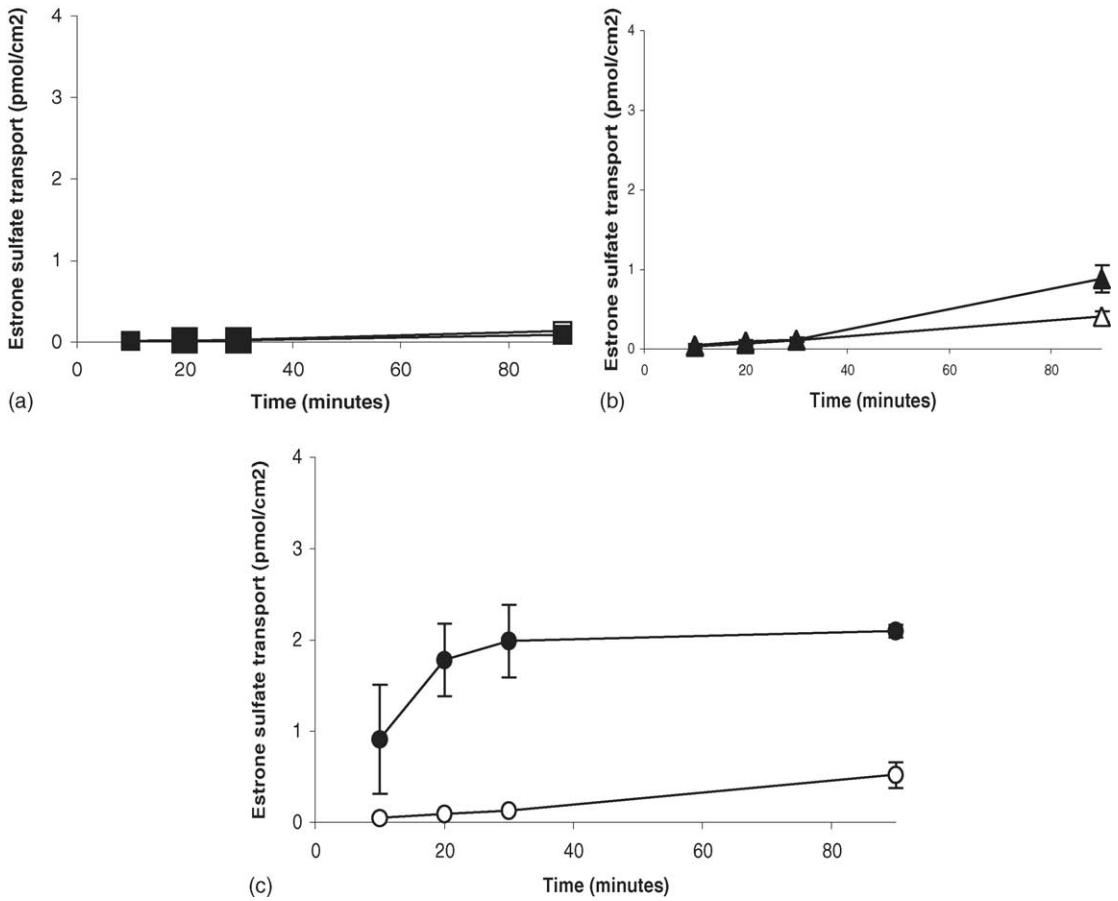

Fig. 4. Time profiles for the transcellular transport of estrone sulfate across LLC-PK1 monolayer. Transcellular transport of [^{3}H]E_1S (1 μM, specific activity: 2.16 Ci/mmol)) across LLC-PK1 monolayers expressing (b) OATP1B1, (c) both OATP1B1 and MRP2 compared with (a) control LLC-PK1 monolayer. Open and closed circles represent the transcellular transport in the apical-to-basal and basal-to-apical directions, respectively. Each point and error bar represents the mean ± S.E. of three determinations. Where error bars are not shown, the S.E. was contained within the limits of the symbol.

(Fig. 2c) and immunofluorescence (data not shown) employing antibodies against the HA-tag did not yield any signals. In addition LLC-PK1 cells contained only low levels of MRP2 as revealed by immunoblotting (Fig. 2c) and as described in our previous study [16]. Immunoblotting and densitometric analysis also revealed that the level of recombinant OATP1B1 and MRP2 was higher than that in human hepatocytes, with the caveat that the liver sample was only derived from one individual. Thus the cell line will be highly useful to predict the OATP1B1 and MRP2-mediated hepato-biliary transport of drugs in qualitative although not quantitative terms.

Immunohistochemistry using confocal laser-scannning microscopy demonstrated a polarised expression of recombinant OATP1B1 and MRP2 in LLC-OATPC/MRP2 cells (Fig. 1) with OATP1B1 being localised baso-laterally as is particularly evident from the z-stacks (note in some parts of the *y*–*z* stack the basal staining for OATP1B1 runs clearly parallel to and below the staining for MRP2). Polarised expression of the two transporters was confirmed by the pronounced directional transport of several substrates in LLC-OATPC/MRP2 cells and demonstrates that OATP1B1 and MRP2 correctly localized to the basolateral and apical membrane respectively. The correct localization of OATP1B1 also shows that the HA-tag did not interfere with the correct cellular sorting of OATP1B1. Furthermore LLC-OATPC/MRP2 cells displayed an apical-to-basolateral transport of $E_2$17βG of 10 pmol/(cm^2 h) (determined from the value at 60 min). With the total cellular protein per cm^2 being typically 0.02 mg (data not shown), this translates into a specific activity 500 pmol/h/mg protein, a value which is in good agreement with data obtained with MDCKII cells which co-expressed OATP1B1 and MRP2 [16]. Based on this observation we also conclude that the presence of a C-terminal HA-tag did not interfere with the function of OATP1B1. It is anticipated that this approach will facilitate the expression of recombinant transporters even in the presence of closely related isoforms. It should be noted that the transcellular transport of $E_2$17βG by LLC-OATPC/MRP2 cells approached saturation at a concentration of 100 μM of this substrate (data not shown). The K_m value for this substrate was reported to be 10 μM with the K_m for DHEAS and E_1S having similar values (reviewed in [2]).

Transport of $E_2$17βG and E_1S in both directions was similar in LLC-PK1 cells. Co-expression of both

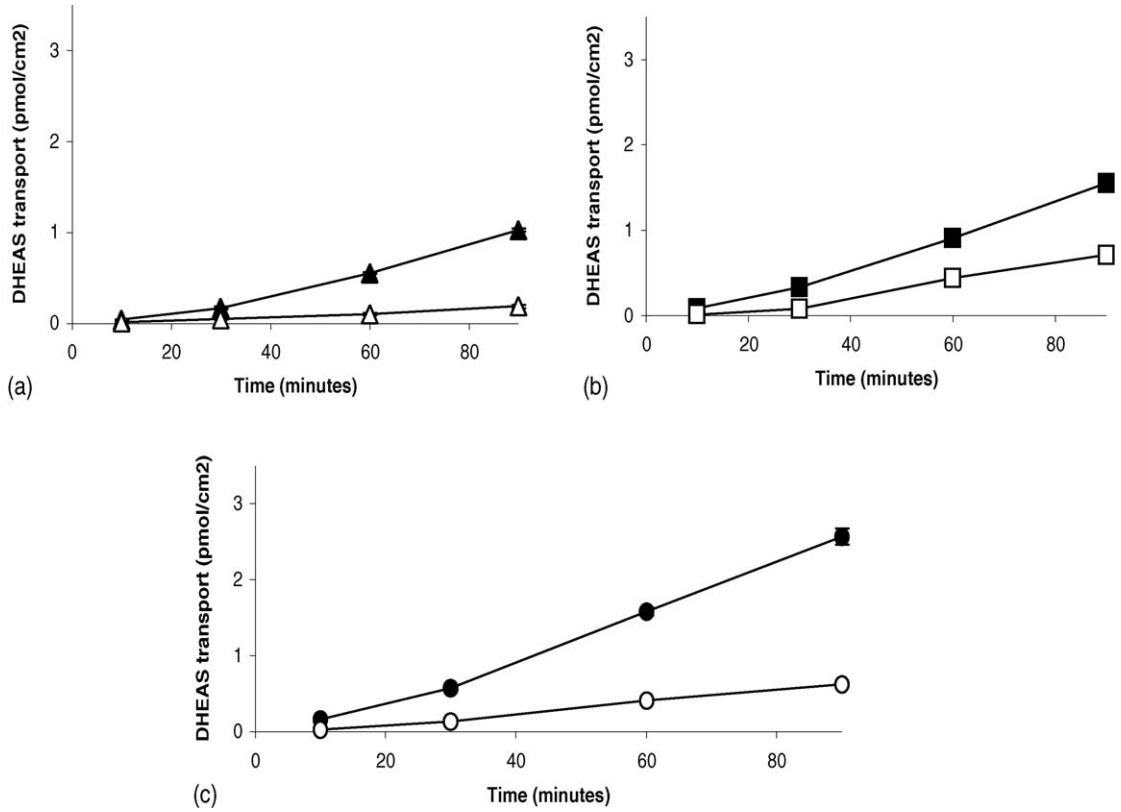

Fig. 5. Time profiles for the transcellular transport of dehydroisoandrosterone-sulfate across LLC-PK1 monolayer. Transcellular transport of [^{3}H]DHEAS (1 μM, specific activity: 3.0 Ci/mmol)) across LLC-PK1 monolayers expressing (b) OATP1B1, (c) both MRP2 and OATP1B1 compared with (a) control LLC-PK1 monolayer. Open and closed circles represent the transcellular transport in the apical-to-basal and basal-to-apical directions, respectively. Each point and error bar represents the mean ± S.E. of three determinations. Where error bars are not shown, the S.E. was contained within the limits of the symbol.

OATP1B1 and MRP2 resulted in a more than 20-fold stimulation of the basolateral-to-apical flux of $E_2$17βG (determined at 60 min time point) and E_1S (determined at 20 min time point) respectively (Figs. 3 and 4). Unlike for $E_2$17βG and DHEAS, the transport of E_1S unexpectedly did not continue beyond 30 min. This unusual time-course was reproduced in a second experiment (data not shown); however, we do not have an explanation for this unusual finding. Mass-spectroscopic analysis confirmed that E_1S had been transported from the basolateral to the apical site and excluded the possibility that the radiometric assay had inadvertently detected the transport of a metabolite being formed intracellularily.

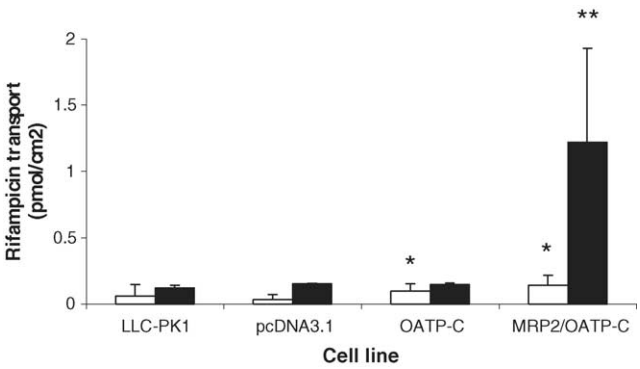

Fig. 6. Transcellular transport of rifampicin (50 μM) across LLC-PK1 monolayers expressing OATP1B1, both OATP1B1 and MRP2, compared with that across the control LLC-PK1 monolayer and LLC-PK1 monolayers containing pcDNA3.1 empty vector. Transport was measured during a 60 min incubation. The concentration of rifampicin after transcellular transport was determined by the specific absorption of rifampicin at 475 nm. Open and closed bars represent the transcellular transport in the apical-to-basal and basal-to-apical directions, respectively. Each point and error bar represents the mean ± S.E. of three determinations. The students *t*-test was performed to compare the values (either apical-to-basal or basal-to-apical directions) obtained for the mock-transfected cells with those obtained for the other cell lines $^*p \leq 0.05$, $^{**}p \leq 0.01$.

It is important to note, that others have found, using the MDCKII-derived cellular model, that co-expression of OATP1B1 and MRP2 did not increase the basolateral-to-apical transport of E_1S and DHEAS compared to cells, which expressed only OATP1B1 [17]. However, LLC-PK1 cells that expressed both transporters displayed a much higher directional transport of E_1S (Fig. 4) and a moderately higher transport of DHEAS (Fig. 5) compared to cells that expressed only OATP1B1. This strongly indicates that the level of endogenous MRP2 in LLC-PK1 cells is distinctly lower than that in MDCKII cells, thus creating less interference of the animal MRP2 with the characterisation of the properties of human MRP2 in transport assays. However, the observation that the transcellular transport of DHEAS, unlike that of the other substrates, was already pronounced in the parental cells may suggest that

LLC-PK1 cells contain proteins, which mediate the transport of this substrate.

The data displayed in Fig. 6 on the trans-epithelial transport of rifampicin, also shows the polarized cell lines that co-express drug uptake and efflux transporters are suitable to investigate the role in the transcellular transport of pharmaceutical drugs. Previously it has been shown that OATP1B3 and MRP2-mediated the transcellular flux of the antibiotic rifampicin across MDCKII cells that co-expressed these transporters [15]. Here we demonstrate that also OATP1B1 together with MRP2 is responsible for the basolateral-to-apical transport of rifampicin. It is unlikely that the slight increase in the flux of rifampicin in the opposite direction upon co-expression of both transporters was due to their incomplete polarized expression, since no similar phenomenon had been noted with $E_2$17βG (Fig. 3).

In conclusion, the data presented herein illustrate that polarized LLCPK-1 cells, which express human drug uptake and efflux transporters are highly suitable to determine their role in transcellular transport. Our data suggest further that, because of lower levels of endogenous ABCC2, LLC-PK1 cells may be more amenable than MDCK-derived models [17] for this purpose. Until recently, the substrate specificity of MRP2 had to be studied employing inside/out vesicles isolated from either liver or recombinant cells which expressed this transporter alone. The latter cells cannot be used to establish MRP2-mediated transport, since most MRP2 substrates cannot enter cells in absence of OATPs. Preparation of vesicles is rather tedious and does not lend itself to high-throughput screening, unlike assays that measure the transcellular transport of xenobiotics. Furthermore, vesicles isolated from liver will contain other transporters that may complicate data interpretation. OATP-mediated uptake can be determined in whole cells, however again this procedure is not suitable for high throughput screening. Polarized recombinant cell lines as models for hepato-biliary transport of pharmaceuticals are also likely to be useful to investigate the interaction of drug transport with drug metabolism, with the former process determining the intracellular concentration of compounds that are substrates or inducers of hepatic P450s. Models to investigate these interactions models can be established either by introducing the relevant P450s in the recombinant cell lines that express human transporters [12] or by employing these cells in reporter assays that measure P450 induction.

Acknowledgments

This work was supported by grants from GlaxoSmith-Kline and Pfizer.

References

[1] Ayrton A, Morgan P. Role of transport proteins in drug absorption, distribution and excretion. Xenobiotica 2001;31:469–97.
[2] Hagenbuch B, Meier PJ. The superfamily of organic anion transporting polypeptides. Biochem Biophys Acta 2003;1609:1–18.
[3] Nishizato Y, Ieiri I, Suzuki H, Kimura M, Kawabata K, Hirota T, et al. Polymorphisms of OATP-C (SLC21A6) and OAT3 (SLC22A8) genes: consequences for pravastatin pharmacokinetics. Clin Pharmacol Ther 2003;73:554–65.
[4] Ishizuka H, Konno K, Naganuma H, Nishimura K, Kouzuki H, Suzuki H, et al. Transport of temocaprilat into rat hepatocytes: role of organic anion transporting polypeptide. J Pharmacol Exp Ther 1998;287(1): 37–42.
[5] Tirona RG, Leake BF, Wolkoff AW, Kim RB. Human organic anion transporting polypeptide-C (SLC21A6) is a major determinant of rifampin-mediated pregnane X receptor activation. J Pharmacol Exp Ther 2003;304:223–8.
[6] Borst P, Evers R, Kool M, Winjholds J. A family of drug transporters: the multidrug resistance-associated proteins. J Natl Cancer Inst 2000;92:1295–302.
[7] Cole SP, Sparks KE, Fraser K, Loe DW, Grant CE, Wilson GM, et al. Pharmacological characterization of multidrug resistance MEP-transfected human tumour cells. Cancer Res 1994;54:5902–10.
[8] Evers R, Kool M, Smith AJ, van Deemter L, de Hans M, Borst P. Inhibitory effect of the reversal agents V-104, GF120918 and Pluronic L61 on MDR1 Pgp-MRP1- and MRP2-mediated transport. Br J Cancer 2000;83:366–74.
[9] Suzuki H, Sugiyama Y. Transporters for bile acids and organic anions. In: Amidon GL, Sadee W, editors. Membrane transporters as drug targets. New York: Kluwer Academic; 1999. p. 387–439.
[10] Rippin SJ, Hagenbuch B, Meier PJ, Stieger B. Cholestatic expression pattern of sinusoidal and canalicular organic anion transport systems in primary cultured rat hepatocytes. Hepatology 2001;33:776–82.
[11] Lee TK, Hammond CL, Ballatori N. Intracellular glutathione regulates taurocholate transport in HepG2 cells. Toxicol Appl Pharmacol 2001;174:207–15.
[12] Baron JM, Goh LB, Yao DG, Wolf CR, Friedberg T. Modulation of P450CYP3A4-dependent metabolism by p-glycoprotein: Implications for P450 phenotyping. J Pharmacol Exp Ther 2001;296:351–8.
[13] König J, Cui Y, Nies AT. A novel human organic anion transporting polypeptide localized to the basolateral hepatocyte membrane. Am J Physiol Gastrointest Liver Physiol 2000;278:G156–64.
[14] Irvine JD, Takahashi L, Lockhart K, Cheong J, Tolan JW, Selick HE, et al. MDCK cells: a tool for membrane permeability screening. J Pharm Sci 1999;88:28–33.
[15] Cui YH, König J, Keppler D. Vectorial transport by double transfected cells expressing the human uptake transporter SLC21A8 and the apical export pump ABCC2. Mol Pharmacol 2001;60:1866–76.
[16] Goh LB, Spears KJ, Yao D, Ayrton A, Morgan P, Wolf CR, et al. Endogenous drug transporters in in vitro and in vivo models for the prediction of drug disposition in man. Biochem Pharmacol 2002;64:1569–78.
[17] Sasaki M, Suzuki H, Ito K, Abe T, Sugiyama Y. Transcellular transport of organic anions across a double-transfected Madin-Darby canine kidney II cell monolayer expressing both human organic anion-transporting polypeptide (OATP2/SLC21A6) and multidrug resistance-associated protein 2 (MRP2/ABCC2). J Biol Chem 2002;277:6497–503.
[18] Kneuer C, Honscha KU, Honscha W. Sodium-dependent methotrexate carrier-1 is expressed in rat kidney: cloning and functional characterization. Am J Physiol Renal Physiol 2004;286:F564–72.